Intermediate-coupling calculations of the effects of interacting resonances on dielectronic recombination in a static electric field

D. C. Griffin
Department of Physics, Rollins College, Winter Park, Florida 32789

D. Mitnik, M. S. Pindzola, and F. Robicheaux
Department of Physics, Auburn University, Auburn, Alabama 36849

(Received 16 July 1998)

Recently, we demonstrated that the enhancement of dielectronic recombination by an electric field, or crossed electric and magnetic fields, may be reduced by the interaction between resonances through a common continuum [Phys. Rev. Lett. **80**, 1402 (1998)]. However, these calculations were carried out in a configuration-average (CA) approximation and the question then remained as to how these predicted reductions might be affected when one removes the degeneracy inherent in the CA approximation and includes the interactions between the resonant states associated with individual intermediate-coupled levels. In the present paper we address that issue for the case of dielectronic recombination in the presence of an electric field. Indeed we have found that these more detailed calculations support the general conclusions of our earlier work and provide additional insight into the effects of interacting resonances on dielectronic recombination in the presence of fields. Results for the Li-like ions C^{3+}, Ne^{7+}, and Si^{11+} are presented. [S1050-2947(98)02712-7]

PACS number(s): 34.80.Lx

I. INTRODUCTION

In recent years there has been a significant number of high-resolution measurements of total electron-impact recombination. In general, these measurements have been in good agreement with theoretical calculations using the independent-processes, isolated-resonance approximation in which one ignores interference effects between radiative recombination and dielectronic recombination (DR) as well as between individual dielectronic resonances. A number of theoretical studies have considered the effects of the interactions between individual resonances [1–9] on dielectronic recombination. However, in the absence of external fields, no one has yet been able to demonstrate clearly that such interactions have any significant effect on total DR.

When there are no external fields, only a small fraction of the total number of resonances can interact with each other through a common electron or photon continuum [5]. In order to interact through the electron continuum, they must have the same parity and the same total angular momentum. In order to couple through the photon continuum, they must differ by no more than two units of angular momentum; in addition, they cannot couple through a core radiative transition unless they also exhibit strong configuration interaction and radiative coupling through the Rydberg electron can be appreciable only for relatively small values of the principal quantum number. Furthermore, those resonances that can interact must be separated by no more than a few times their natural widths in order to show any appreciable interference effects [5]. All these factors significantly limit the importance of interacting resonances on total DR in a field-free environment.

With the introduction of static fields, things change significantly. It is now well known that an external electric field can cause a large enhancement of DR. This is due to the fact that the probability of recombination into doubly excited Rydberg states decreases rapidly with the angular momentum l of the Rydberg electron. However, the electric field mixes Rydberg states that differ in l by one; this redistribution of angular momentum then opens up many more channels for recombination and thereby increases the DR cross section. More recently it has been demonstrated that additional enhancement of DR occurs with crossed electric and magnetic fields [10,11]. In the presence of an electric or a magnetic field alone or parallel electric and magnetic fields, M is a good quantum number and the probability of recombination falls off rapidly with M. However, when the magnetic field has a component perpendicular to the electric field, states that differ in M by one mix; this redistribution of magnetic quantum numbers opens up still more channels for recombination and further enhances the DR cross section.

This mixing of states in the presence of fields can also cause a significant increase in the interaction between dielectronic resonances through a common continuum. For example, since the electric field mixes states of opposite parity and states that differ by one in the total angular momentum, many more states can interact through a common continuum. Furthermore, the field-mixed states in the presence of relatively small electric fields are sufficiently closely spaced that many of the resonances are overlapping (i.e., their widths are larger than the energy spacing).

Indeed, in an earlier study [12], we employed a configuration-average (CA) approximation to demonstrate that interactions through common continuua can substantially reduce the enhancement of DR by electric and crossed electric and magnetic fields. However, all the levels of a given doubly excited configuration are treated as a single entity in these CA calculations; therefore, they do not include the interactions between the resonant states associated with individual levels. It was then essential to examine how the removal of this degeneracy between levels of a configuration would affect the magnitude of these interactions and thereby our general conclusions regarding the importance of interfering resonances to field-enhanced DR. In this paper we

have done that by considering the effects of interacting resonances on dielectronic recombination in an electric field, using a full level-to-level intermediate-coupling (IC) approach.

The remainder of this paper is arranged as follows. In the next section we present a summary of the theoretical methods that are employed. In Sec. III we consider the Li-like ions C^{3+}, Ne^{7+}, and Si^{11+} and present the results of our intermediate-coupled total DR cross section calculations for these ions with and without the inclusion of interacting resonances. We also compare our IC results for C^{3+} and Si^{11+} with our earlier CA DR cross sections. Finally, in Sec. IV, we summarize our findings and discuss their implications.

II. THEORETICAL METHODS

In our earlier paper on this subject [12] we gave a brief development of interacting resonance theory leading to the calculation of dielectronic recombination in the CA approximation. Here we repeat that theoretical development, focusing on the specific form of these equations that applies to our present treatment of the individual doubly excited levels in intermediate coupling.

We employ the projection operator technique [13,14] in which the Schrödinger equation may be written as three coupled equations

$$(E-PH_0P)P\Psi=PVQQ\Psi, \tag{1}$$

$$(E-QH_0Q-QVQ)Q\Psi=QVPP\Psi+QDRR\Psi, \tag{2}$$

$$(E-RH_0R)R\Psi=RDQQ\Psi, \tag{3}$$

where the total Hamiltonian $H=H_0+V+D$ and the projection operators $P+Q+R=1$. The Hamiltonian H_0 represents the electron-nuclear interactions and the configuration-average portion of the electron-electron interactions; V includes the residual electron-electron interactions, the spin-orbit interactions, and the electron interactions with the external electric field; and D represents the interaction of the electrons with the radiation field, which in the dipole approximation is given by $D=\sqrt{2\omega^3/3\pi c^3}\Sigma_i\vec{r}_i$, where ω is the frequency of the emitted radiation and c is the speed of light.

P projects onto states of N bound electrons, one continuum electron, and no photons and is expanded in a basis set consisting of the solutions to the configuration-average Hartree-Fock (CAHF) equations for the N bound electrons and the configuration-average distorted-wave (CADW) equations for the continuum electron. Q projects onto doubly excited autoionizing states of $N+1$ ''bound'' electrons and no photons and is expanded in a basis set consisting of the solutions to the CAHF equations for these autoionizing states. Finally, R projects onto the ground and bound excited states of $N+1$ bound electrons and one photon and is expanded in a basis set consisting of the solutions to the CAHF equations for these states. In Eq. (1) we have ignored continuum-continuum coupling either by the electron-electron interaction ($PVP=0$) or the radiation field ($PDP=0$) since we employ distorted waves. In addition, we have not included the coupling of the continuum channels directly to the $N+1$ bound electrons in either Eq. (1) ($PDR=0$) or Eq. (3) ($RDP=0$) since we are not interested in radiative recombination. In Eq. (2) we also ignore cascades among the doubly excited autoionizing levels ($QDQ=0$). Finally, in Eq. (3) we ignore the detailed level structure of the bound electrons ($RVR=0$), although in the case of the Li-like ions considered here, we do correct the energies of the doubly excited bound levels of the type $2pnl$ for the spin-orbit interaction of the $2p$ electron.

We see from Eq. (1) that $P\Psi=P\psi^+ +(E-PH_0P)^{-1}PVQQ\Psi$ and from Eq. (3) that $R\Psi=(E-RH_0R)^{-1}RDQQ\Psi$; thus we may formally solve for $Q\Psi$ by substituting these into Eq. (2):

$$Q\Psi=(E-\tilde{H})^{-1}QVP\psi^+. \tag{4}$$

Here the Hamiltonian $\tilde{H}$ is given by

$$\tilde{H}=QH_0Q+QVQ+QVP(E-PH_0P)^{-1}PVQ + QDR(E-RH_0R)^{-1}RDQ \tag{5}$$

and ψ^+ is a wave function consisting of CAHF solutions for the N bound electrons plus a CADW solution for the continuum electron, which satisfies the outgoing-wave boundary conditions; in the above notation, ψ^+ corresponds to the homogeneous solution of Eq. (1). The matrix element for DR is given by

$$\mathcal{M}=\langle\chi|RDQ|Q\Psi\rangle, \tag{6}$$

where χ is a solution to the CAHF equations for the final $(N+1)$-electron bound states; in the above notation, it corresponds to the homogeneous solution of Eq. (3). Substituting Eq. (4) into Eq. (6), we find that the matrix element for DR from a state i of the initial level plus the continuum electron to a final bound state f is given by

$$\mathcal{M}_{fi}=\langle\chi_f|RDQ(E-\tilde{H})^{-1}QVP|\psi_i^+\rangle. \tag{7}$$

The DR cross section is proportional to $|\mathcal{M}_{fi}|^2$. However, before applying this equation, we must first analyze the Hamiltonian $\tilde{H}$ in terms of a basis set of the doubly excited autoionizing states. We choose the set $|\phi_\alpha\rangle$, which consists of the solutions of the configuration-average Hartree-Fock equation

$$(E-QH_0Q)|\phi_\alpha\rangle=0, \tag{8}$$

and in our work will be represented in pure j-K coupling for each of the degenerate levels α of a given doubly excited configuration. In the pole approximation for outgoing waves, we may express the matrix elements of $\tilde{H}$ in this basis set in terms of the generalized autoionizing rates $\Gamma^a_{\alpha\beta}$ and the generalized radiative rates $\Gamma^r_{\alpha\beta}$ as

$$\langle\phi_\alpha|\tilde{H}|\phi_\beta\rangle\equiv\tilde{H}_{\alpha\beta}=E_\alpha\delta_{\alpha,\beta}+V_{\alpha\beta}-\frac{i}{2}(\Gamma^a_{\alpha\beta}+\Gamma^r_{\alpha\beta}) \quad , \tag{9}$$

where

$$\Gamma^a_{\alpha\beta}=\frac{4}{k}\sum_i \langle\phi_\alpha|QVP|\psi_i^+\rangle\langle\psi_i^+|PVQ|\phi_\beta\rangle \tag{10}$$

and

$$\Gamma^r_{\alpha\beta}=2\pi\sum_f \langle\phi_\alpha|QDR|\chi_f\rangle\langle\chi_f|RDQ|\phi_\beta\rangle. \quad (11)$$

In Eq. (10) the continuum wave function is normalized to one times a sine function and k is the linear momentum of the continuum electron. The diagonal elements of $\Gamma^a_{\alpha\beta}$ and $\Gamma^r_{\alpha\beta}$ are the total autoionization and total radiative rates in atomic units evaluated in pure j-K coupling; it is important to note that they do not include the effects of intermediate coupling or field mixing. The DR cross section to go from state i to state f may then be written as

$$\sigma^{f\leftarrow i}_{DR}(E)=\frac{8\pi^2}{k^3}\left|\sum_{\alpha,\beta} D_{f\alpha}[(E-\tilde{H})^{-1}]_{\alpha\beta}V_{\beta i}\right|^2, \quad (12)$$

where $D_{f\alpha}=\langle\chi_f|RDQ|\phi_\alpha\rangle$ and $V_{\beta i}=\langle\phi_\beta|QVP|\psi_i^+\rangle$.

We now consider the eigenvalues and eigenvectors of the complex matrix $\tilde{H}_{\alpha\beta}$:

$$\sum_\beta \tilde{H}_{\alpha\beta}U_{\beta\rho}=U_{\alpha\rho}\tilde{E}_\rho. \quad (13)$$

Since $\tilde{H}_{\alpha\beta}$ is not Hermitian, the eigenvalues will be complex and with the outgoing wave boundary conditions, the imaginary part of the eigenvalues will be negative. However, since $\tilde{H}_{\alpha\beta}$ is symmetric, the eigenvectors must be orthogonal and they can also be normalized to one so that $\Sigma_\beta U_{\beta\rho}U_{\beta\rho'}=\delta_{\rho\rho'}$. Furthermore, the closure relationship is $\Sigma_\rho U_{\alpha\rho}U_{\beta\rho}=\delta_{\alpha\beta}$. One can now transform the Green's function to the space described by the complex eigenvalues and eigenvectors of Eq. (12) using the equation

$$(E-\tilde{H})^{-1}_{\alpha\beta}=\sum_{\rho,\rho'} U_{\alpha\rho}(E-\tilde{H})^{-1}_{\rho\rho'}U_{\beta\rho'}$$
$$=\sum_{\rho,\rho'} U_{\alpha\rho}(E-\tilde{E}_\rho)^{-1}\delta_{\rho\rho'}U_{\beta\rho'}. \quad (14)$$

We then obtain the expression for the cross section

$$\sigma^{f\leftarrow i}_{DR}(E)=\frac{8\pi^2}{k^3}\left|\sum_\rho D_{f\rho}(E-\tilde{E}_\rho)^{-1}V_{\rho i}\right|^2, \quad (15)$$

where $D_{f\rho}=\Sigma_\alpha D_{f\alpha}U_{\alpha\rho}$ and $V_{\rho i}=\Sigma_\beta V_{\beta i}U_{\beta\rho}$. In order to evaluate the total DR cross section from the initial level of the ion, we sum over the final bound states f of the $(N+1)$-electron ion and average over the initial states of the N-electron ion plus the continuum electron to obtain

$$\sigma^{tot}_{DR}(E)=\frac{\pi}{2gk^2}\sum_{\rho,\rho'}\frac{\Gamma^a_{\rho\rho'}\Gamma^r_{\rho\rho'}}{(E-\tilde{E}^*_{\rho'})(E-\tilde{E}_\rho)}, \quad (16)$$

where g is the statistical weight of the initial level of the ion, the factor of 2 in the denominator is the statistical weight of the continuum electron, and $\Gamma^a_{\rho\rho'}$ and $\Gamma^r_{\rho\rho'}$ are the generalized autoionizing and radiative rates, respectively, evaluated in the basis set formed from the eigenvectors of $\tilde{H}_{\alpha\beta}$. They are given by

$$\Gamma^a_{\rho\rho'}=\frac{4}{k}\sum_i V^*_{\rho' i}V_{\rho i}=\sum_{\alpha,\beta} U^*_{\beta\rho'}U_{\alpha\rho}\Gamma^a_{\alpha\beta} \quad (17)$$

and

$$\Gamma^r_{\rho\rho'}=2\pi\sum_f D^*_{\rho' f}D_{\rho f}=\sum_{\alpha,\beta} U^*_{\beta\rho'}U_{\alpha\rho}\Gamma^r_{\alpha\beta} \quad (18)$$

and are complex and include the effects of intermediate coupling, electric-field mixing, and interacting resonances [15].

Finally, we convolute this total cross section with a weight function $W(E,E_0)$, which has an energy width much greater than the imaginary parts of E_ρ:

$$\langle\sigma^{tot}_{DR}\rangle(E_0)=\int \sigma^{tot}_{DR}(E)W(E,E_0)dE. \quad (19)$$

In using the residue theorem to evaluate this integral, we average over two possible contour integrals, one in the upper half, of the complex plane and the other in the lower half, to obtain the approximate result

$$\langle\sigma^{tot}_{DR}\rangle(E_0)\simeq\frac{\pi^2 i}{gk^2}\sum_{\rho,\rho'}\Gamma^a_{\rho\rho'}\Gamma^r_{\rho\rho'}$$
$$\times W(\tfrac{1}{2}\,\mathrm{Re}[\tilde{E}_\rho+\tilde{E}_{\rho'}],E_0)/(\tilde{E}^*_{\rho'}-\tilde{E}_\rho). \quad (20)$$

In this paper we will present the results of the total cross section integrated over the energy of the doubly excited states of a particular prinicipal quantum number n of the Rydberg electron. To do this we use a weight function of width ΔE larger than the largest energy spread of the doubly excited states within any n manifold and with a constant magnitude equal to $1/\Delta E$. We then obtain the following result for $\sigma\Delta E$:

$$\langle\sigma^{n,tot}_{DR}\rangle\Delta E=\frac{\pi^2 i}{gk^2}\sum_{\rho,\rho'}\Gamma^a_{\rho\rho'}\Gamma^r_{\rho\rho'}/(\tilde{E}^*_{\rho'}-\tilde{E}_\rho), \quad (21)$$

where the double sum over ρ and ρ' is now over all eigenvectors of $\tilde{H}_{\alpha\beta}$ within a given n manifold. Although it is not obvious from this equation, it is quite straightforward to show that the double sum in Eq. (21) is purely imaginary so that the cross section will be real, as required.

Equation (21) is the primary working equation of this paper; however, for comparison we have also evaluated the total DR cross sections for a given value of n using the isolated resonance approximation

$$\langle\sigma^{n,tot}_{DR}\rangle\ \Delta E=\frac{\pi^2}{gk^2}\sum_j A^a_j A^r_j/(A^a_j+A^r_j), \quad (22)$$

where the sum over j is over all doubly excited resonant states within the n manifold. Here we use the symbols A^a_j and A^r_j to represent the intermediate-coupled, electric-field mixed autoionizing and radiative rates for a given doubly excited resonance state j; they are calculated in the isolated resonance approximation from the expressions

$$A^a_j=\frac{4}{k}\sum_i\left|\sum_\beta Y_{\beta j}V_{\beta i}\right|^2=\sum_{\alpha,\beta} Y_{\beta j}Y_{\alpha j}\Gamma^a_{\alpha\beta}, \quad (23)$$

$$A_j^r = 2\pi \sum_f \left| \sum_\beta Y_{\beta j} D_{f\beta} \right|^2 = \sum_{\alpha,\beta} Y_{\beta j} Y_{\alpha j} \Gamma^r_{\alpha\beta}, \qquad (24)$$

where $Y_{\beta j}$ are the real eigenvectors of the Hamiltonian with matrix elements given by the real parts of Eq. (9).

It should be pointed out that for simplicity in the above equations, we have not distinguished between the total autoionizing rates to the states of the initial level of the *N*-electron ion and the total rates to the states of all lower levels of the *N*-electron ion. However, for the Li-like ions considered here, the only autoionizing transitions are to the single initial level $2s\,^2S_{1/2}$ since we do not include values of n high enough that the intercombination transitions from $2p_{3/2}nl$ to $2p_{1/2}$ are possible. The programs that we employ to make these calculations do make these distinctions and therefore can be applied to a more general case.

We have carried out calculations of total DR in an electric field in the isolated-resonance approximation from Eq. (22) using our program DRFEUD, which is described in detail by Griffin *et al.* [16]. We have also developed a modified version of that program to perform calculations of total DR in an electric field with the inclusion of interacting resonances using Eq. (21).

The calculations performed using interacting-resonance theory are tractable in the presence of an electric field, even though one must repeatedly diagonalize a complex Hamiltonian for each possible value of the magnetic quantum number *M*. However, we are not able to consider similar calculations in the presence of crossed electric and magnetic fields. The reason is that since *M* is no longer a good quantum number, the matrices that must be diagonalized using a full IC approach are extremely large [11], and performing diagonalizations of a complex Hamiltonian for such a system is not feasible at the present time. However, these IC, electric-field calculations should shed some light on the validity of our earlier CA, interacting-resonance theory calculations of DR in the presence of crossed electric and magnetic fields [12].

III. RESULTS OF CALCULATIONS

We now present our results for the Li-like ions C^{3+}, Ne^{7+}, and Si^{11+}. The ions C^{3+} and Si^{11+} were considered in our CA calculations [12] and Ne^{7+} was added in order to provide more detail regarding the variation of these effects as a function of ionization stage.

In Fig. 1 we show the values for $\langle \sigma_{DR}^{n,tot} \rangle\ \Delta E$ for C^{3+} calculated using Eqs. (21) and (22) as a function of n for electric fields of 2 V/cm and 20 V/cm. For comparison, we also display the no-field results, calculated in the isolated-resonance approximation. We see that with a relatively small electric field of 2 V/cm, the quantity $\langle \sigma_{DR}^{n,tot} \rangle \Delta E$, calculated in the isolated-resonance approximation, increases rapidly with n from $n=12$ to $n=22$ and then increases more gradually up to about $n=30$, where it begins increasing more rapidly again. However, the values of $\langle \sigma_{DR}^{n,tot} \rangle\ \Delta E$, calculated with the inclusion of interacting resonances, are significantly reduced compared to the isolated-resonance values and they increase very gradually throughout this range of n. The reduction due to the effects of interacting resonances is about 40% at $n=40$. However, when the field is increased to 20 V/cm, the effects of interacting resoances are much less dramatic and the reduction at $n=40$ for this field is only about 17%. In general, as the electric field becomes larger, the significance of the interactions between the resonances is reduced; the states are sufficiently spread out in energy by the larger field that fewer of the resonances are overlapping.

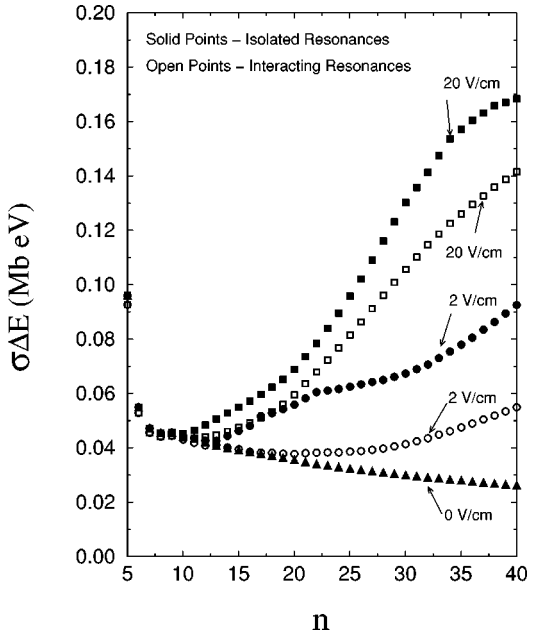

FIG. 1. Total dielectronic recombination cross section times the energy-bin width as a function of n for C^{3+} from an IC calculation. Solid triangles, isolated resonances and no fields; open circles, interacting resonances and an electric field of 2 V/cm; solid circles, isolated resonances and an electric field of 2 V/cm; open squares, interacting resonances and an electric field of 20 V/cm; solid squares, isolated resonances and an electric field of 20 V/cm.

Another way to demonstrate these effects as a function of field strength is provided in Table I. There we give the values of $\langle \sigma_{DR}^{tot} \rangle\ \Delta E$ for C^{3+}, integrated over an energy range from $n=25$ to $n=38$ as a function of electric-field strength. We show separately in this table the results for the $2p_{1/2}nl$ and $2p_{3/2}nl$ resonances as well as the totals. Finally, we compare our results with those obtained from the CA approximation in Ref. [12]. We first see that, in the absence of the electric field, the effects of interacting resonances are of the order of 2–3 %. These very small effects are what we would expect on the basis of the arguments presented in Sec. I.

These integrated values of $\langle \sigma_{DR}^{tot} \rangle\ \Delta E$, calculated in the isolated-resonance approximation, for the $2p_{1/2}nl$ and $2p_{3/2}nl$ resonances show quite different behavior as a function of electric-field strength. In the case of the $2p_{1/2}nl$ resonances, the cross section increases dramatically as the field is increased from 0 V/cm to 2V/cm and then increases only slightly as the field strength is further increased. On the other hand, the cross section for the $2p_{3/2}nl$ resonances increases rather gradually with field strength. This difference in behavior as a function of electric field is due solely to the differences in the atomic structure of these two sets of resonances. The $2p_{3/2}nl$ levels are spread out by the direct electrostatic quadrupole interaction as well as the smaller exchange terms and the spin-orbit interaction of the nl electron. However,

TABLE I. DR cross section times the energy-bin width for C^{3+} integrated over an energy including all states from $n=25$ to $n=38$. The σ^r are from the isolated-resonance approximation, while the σ^c include interacting resonances. The CA results are from Ref. [12].

	IC calculations								
F	$\sigma^r\Delta E$ (Mb eV)			$\sigma^c\Delta E$ (Mb eV)			$\sigma^c\Delta E/\sigma^r\Delta E$		
(V/cm)	$2p_{1/2}$	$2p_{3/2}$	Total	$2p_{1/2}$	$2p_{3/2}$	Total	$2p_{1/2}$	$2p_{3/2}$	Total
0	0.139	0.274	0.412	0.136	0.265	0.401	0.98	0.97	0.97
2	0.618	0.387	1.005	0.272	0.342	0.614	0.44	0.88	0.61
4	0.638	0.561	1.199	0.366	0.463	0.828	0.57	0.83	0.69
6	0.649	0.707	1.356	0.421	0.570	0.991	0.66	0.81	0.73
8	0.656	0.826	1.482	0.459	0.659	1.118	0.70	0.80	0.75
10	0.661	0.929	1.590	0.487	0.735	1.222	0.74	0.79	0.77
15	0.670	1.107	1.777	0.533	0.882	1.415	0.80	0.80	0.80
20	0.677	1.224	1.901	0.563	0.989	1.552	0.83	0.81	0.82

	CA results: totals		
F (V/cm)	$\sigma^r\Delta E$ (Mb eV)	$\sigma^c\Delta E$ (Mb eV)	$\sigma^c\Delta E/\sigma^r\Delta E$
0	0.50	0.50	1.00
2	2.18	1.05	0.48
4	2.21	1.43	0.65
6	2.22	1.65	0.74
8	2.23	1.79	0.80
10	2.24	1.88	0.84
15	2.25	2.02	0.90
20	2.26	2.09	0.92

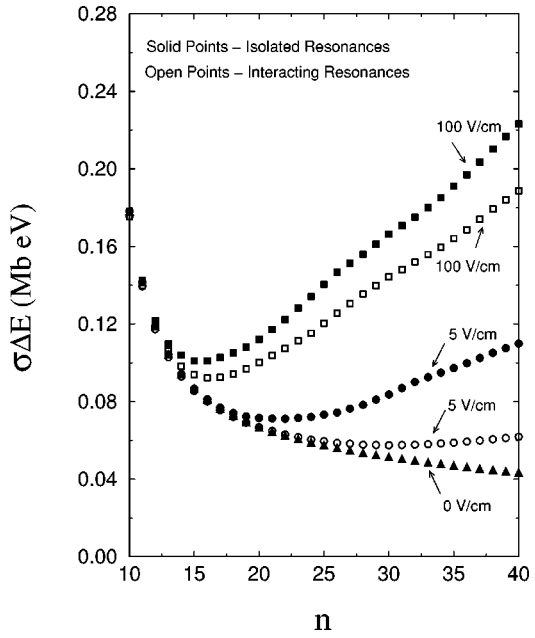

FIG. 2. Total dielectronic recombination cross section times the energy-bin width as a function of n for Ne^{7+} from an IC calculation. Solid triangles, isolated resonances and no fields; open circles, interacting resonances and an electric field of 5 V/cm; solid circles, isolated resonances and an electric field of 5 V/cm; open squares, interacting resonances and an electric field of 100 V/cm; solid squares, isolated resonances and an electric field of 100 V/cm.

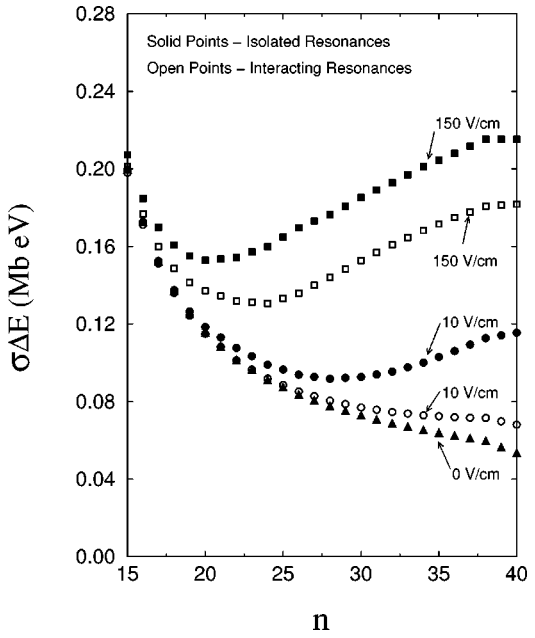

FIG. 3. Total dielectronic recombination cross section times the energy-bin width as a function of n for Si^{11+} from an IC calculation. Solid triangles, isolated resonances and no fields; open circles, interacting resonances and an electric field of 10 V/cm; solid circles, isolated resonances and an electric field of 10 V/cm; open squares, interacting resonances and an electric field of 150 V/cm; solid squares, isolated resonances and an electric field of 150 V/cm.

TABLE II. Same as Table I, but for Ne^{7+}; there are no CA results for this case.

	IC calculations								
F	$\sigma^r\Delta E$ (Mb eV)			$\sigma^c\Delta E$ (Mb eV)			$\sigma^c\Delta E/\sigma^r\Delta E$		
(V/cm)	$2p_{1/2}$	$2p_{3/2}$	Total	$2p_{1/2}$	$2p_{3/2}$	Total	$2p_{1/2}$	$2p_{3/2}$	Total
0	0.235	0.471	0.706	0.232	0.463	0.695	0.99	0.98	0.98
5	0.672	0.564	1.236	0.308	0.512	0.820	0.46	0.91	0.66
10	0.779	0.701	1.480	0.394	0.597	0.991	0.51	0.85	0.67
15	0.821	0.814	1.635	0.460	0.683	1.143	0.56	0.84	0.70
25	0.850	0.985	1.835	0.549	0.830	1.379	0.65	0.84	0.75
50	0.872	1.244	2.116	0.660	1.075	1.735	0.76	0.86	0.82
75	0.882	1.415	2.296	0.715	1.229	1.944	0.81	0.87	0.83
100	0.888	1.547	2.435	0.751	1.347	2.098	0.85	0.87	0.86

there is no direct quadrupole interaction within the $2p_{1/2}nl$ levels; thus these resonances are much more nearly degenerate and a very small electric field will have a pronounced effect on the DR cross section for these resonances. We also see from the lower portion of Table I that a similar variation with field strength is displayed by the CA cross sections, calculated in the isolated-resonance approximation. This would be expected since the levels of $2pnl$ are completely degenerate in the CA approximation.

We also see from this table that the effects of interacting resonances are more pronounced for the $2p_{1/2}nl$ resonances than for the $2p_{3/2}nl$ resonances for all but the highest two field strengths; in fact, at 2 V/cm, the reduction in the cross section due to interacting resonances is about 56% for the $2p_{1/2}nl$ resonances as compared to only 12% for the $2p_{3/2}nl$ resonances. This is again due to the fact that the $2p_{1/2}nl$ resonances are more nearly degenerate, leading to many more overlapping resonances than in the case of the $2p_{3/2}nl$ resonances. These data also show how the effects of interacting resonances become less significant as the field strength increases.

Although we originally predicted that the effect of interacting resonances might be less pronounced in a full IC calculation than in a CA calculation [12], as can be seen from Table I, this is only true at the lowest two field strengths. At the higher field strengths the effect is actually larger in these much more detailed calculations.

In Figs. 2 and 3 we show our values of $\langle\sigma_{DR}^{n,tot}\rangle\Delta E$ as a function of n for Ne^{7+} and Si^{11+}. The Stark matrix elements tend to go off as the inverse of the charge of the ion, while

TABLE III. Same as Table I but for Si^{11+}.

	IC calculations								
F	$\sigma^r\Delta E$ (Mb eV)			$\sigma^c\Delta E$ (Mb eV)			$\sigma^c\Delta E/\sigma^r\Delta E$		
(V/cm)	$2p_{1/2}$	$2p_{3/2}$	Total	$2p_{1/2}$	$2p_{3/2}$	Total	$2p_{1/2}$	$2p_{3/2}$	Total
0	0.328	0.668	0.996	0.326	0.661	0.987	0.99	0.99	0.99
10	0.544	0.834	1.378	0.370	0.708	1.078	0.68	0.85	0.78
20	0.696	0.986	1.682	0.432	0.782	1.214	0.62	0.79	0.72
30	0.793	1.094	1.886	0.491	0.860	1.351	0.62	0.79	0.73
40	0.853	1.178	2.031	0.540	0.934	1.474	0.63	0.79	0.73
50	0.895	1.248	2.143	0.582	1.001	1.583	0.65	0.80	0.74
75	0.954	1.385	2.339	0.663	1.142	1.805	0.69	0.82	0.77
100	0.985	1.492	2.477	0.720	1.252	1.972	0.73	0.84	0.80
150	1.017	1.653	2.669	0.795	1.415	2.210	0.78	0.86	0.83

	CA results: totals		
F	$\sigma^r\Delta E$	$\sigma^c\Delta E$	
(V/cm)	(Mb eV)	(Mb eV)	$\sigma^c\Delta E/\sigma^r\Delta E$
0	1.25	1.25	1.00
10	1.51	1.39	0.92
20	1.95	1.64	0.84
30	2.31	1.89	0.82
40	2.57	2.12	0.82
50	2.77	2.31	0.83
75	3.09	2.67	0.86
100	3.27	2.90	0.89
150	3.46	3.18	0.92

the separation of levels with different l and the same n and the electron-electron matrix elements tend to increase linearly with the charge of the ion; finally, the spin-orbit interaction tends to increase as the fourth power of the ion charge [17]. Thus we have used larger fields as we consider more highly ionized species in order to show comparable effects. In the case of Ne^{7+} we compare results for fields of 5 V/cm and 100 V/cm, while for Si^{11+} we compare results for fields of 10 V/cm and 150 V/cm. We see that these curves are quite similar to those in Fig. 1 for C^{3+}; the primary difference is that, at the lowest field strength, we do not see the rapid increase in the isolated resonances values of $\langle \sigma_{DR}^{n,tot} \rangle \Delta E$ in the lower values of n that is seen in the case of C^{3+}. Again the effect of interfering resonances in these ions is much more pronounced at the lower field strengths.

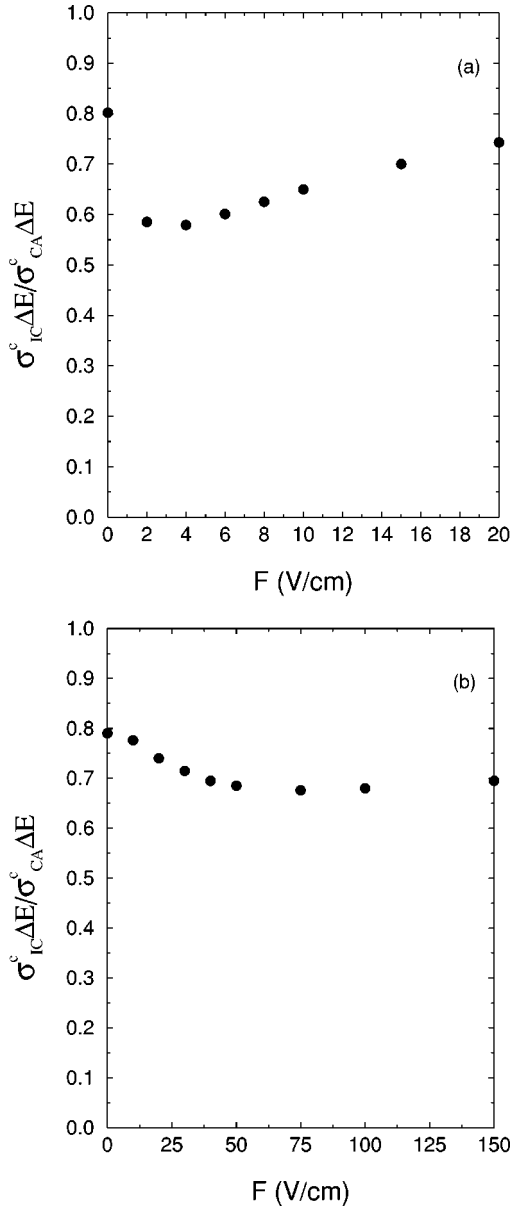

FIG. 4. Ratios $\sigma_{IC}^c \Delta E / \sigma_{CA}^c \Delta E$ (where the the cross sections are integrated over an energy including all states from $n=25$ to $n=38$) as a function of electric-field strength F. The ratios in (a) are for C^{3+} and are calculated from the data given in Table I, while the ratios in (b) are for Si^{11+} and are calculated from the data given in Table III.

In Tables II and III we present the values of $\langle \sigma_{DR}^{tot} \rangle \Delta E$ for Ne^{7+} and Si^{11+}, again integrated over an energy range from $n=25$ to $n=38$, as a function of electric-field strength. In these two ions, interacting resonances reduce the cross section by only about 1% in the absence of a field. We also see a more gradual increase in the isolated resonances cross sections for the $2p_{1/2}nl$ resonances with field strength, especially in the case of Si^{11+}. This is primarily due to the fact that the $2p_{1/2}nl$ resonances are somewhat less degenerate for higher charge states. However, in both of these ions, the effects of interacting resonances remain more pronounced for the $2p_{1/2}nl$ resonances than for the $2p_{3/2}nl$ resonances. We also see in Table III that the CA isolated-resonances cross sections for Si^{11+} increase much more gradually with field strength than is the case for C^{3+}; this is due to the increase with charge state in the separation between doubly excited configurations with the same value of n and different values of l. Finally, we see from Table III that in Si^{11+} the effects of interacting resonances, calculated in the IC approximation, are more significant than for those calculated in the CA approximation at all field strengths.

In order to provide a final comparison of our IC calculations with our earlier CA calculations, we show in Fig. 4 the ratios $\sigma_{IC}^c \Delta E / \sigma_{CA}^c \Delta E$, integrated over an energy range including all states from $n=25$ to $n=38$, as a function of the electric-field strength. The results in Fig. 4(a) are for C^{3+} and were calculated from the data in Table I, while the results in Fig. 4(b) are for Si^{11+} and were calculated from the data in Table III. As can be seen, the variation of these ratios with field strength is more significant for C^{3+}; this might be expected since DR cross sections are more sensitive to the details of the level structure for lower stages of ionization. It is well known that in the absence of fields and in the isolated resonance approximation, CA calculations often overestimate total DR cross sections; with the inclusion of electric fields and interacting resonances this becomes somewhat more pronounced.

IV. CONCLUSIONS

Although our earlier work using the CA approximation predicted that interacting resonances would significantly reduce the enhancement of DR by static fields, it was essential that the magnitude of these effects be investgated using a full IC approach. This has now been accomplished for the case of DR for Li-like ions in a static electric field; the effects are found to be even larger than were indicated by our earlier CA calculations, except for the lowest fields in the lowest charge state considered. As the electric-field strength is increased, the magnitude of the effects of interacting resonances decreases; however, it does so rather gradually. Thus it is only in the presence of very strong electric fields that we would expect the isolated-resonance approximation to provide accurate estimates of electric-field enhanced DR in these ions.

Furthermore, we have discovered that the effects of interacting resonances are much more significant in the more nearly degenerate $2p_{1/2}nl$ resonances than in the $2p_{3/2}nl$ resonances, where the direct quadrupole interaction causes a wider energy spread. This suggests that in those ionic sys-

tems where the levels of a given doubly excited configuration are more uniformly spread out, the effects of interacting resonances may reduced from what we have determined for these Li-like ions. However, the inclusion of electric field mixing and interacting resonance theory in calculations of DR in more complex ionic species, where there may be less degeneracy in the levels, would be a very formidable task indeed.

Because of the size of the complex matrices involve, we are not able to investigate these effects in Li-like ions for crossed electric and magnetic fields. Our earlier work using the CA approximation shows that the size of the reduction due to interacting resonances is more significant when a crossed magnetic field is included. Based on our present work with an electric field, we would predict that these CA calculations give a lower limit to the size of the reductions in crossed fields and a full IC calculation for this case would lead to even larger reductions. Furthermore, one might expect from the ratios given in Fig. 4 for DR in the presence of an electric field alone that the actual magnitude of the CA DR cross sections for Li-like ions in the presence of crossed fields might be reduced by about 25–40 % if a full IC calculation could be peformed, depending on the charge state and the strength of the fields.

This all demonstrates that detailed theoretical analyses of ongoing experiments of DR in storage rings remain a formidable problem in atomic physics. In all of these experiments there are crossed electric and magnetic fields in the interaction region. A complete theoretical analysis would then require a full intermediate-coupling calculation with the inclusion of interacting resonances and crossed electric and magnetic fields. Even if this is accomplished, the problem of determining how these recombined ions evolve before entering the analysis region, where they are field ionized, will continue to complicate the situation [18].

ACKNOWLEDGMENTS

This work was supported by the U.S. Department of Energy (DOE), Office of Fusion Energy, under Contract No. DE-FG05-93ER54218 with Rollins College, Contract No. DE-FG05-86ER53217 with Auburn University, and U.S. DOE EPSCOR Grant No. DE-FC02-91ER75678 with Auburn University.

[1] P. C. W. Davies and M. J. Seaton, J. Phys. B **2**, 757 (1969).
[2] R. H. Bell and M. J. Seaton, J. Phys. B **18**, 1589 (1985).
[3] K. J. LaGattuta, Phys. Rev. A **36**, 4662 (1987).
[4] S. L. Haan and V. L. Jacobs, Phys. Rev. A **40**, 80 (1989).
[5] M. S. Pindzola, N. R. Badnell, and D. C. Griffin, Phys. Rev. A **46**, 5725 (1992).
[6] S. N. Nahar and A. K. Pradhan, Phys. Rev. Lett. **68**, 1488 (1992).
[7] F. Robicheaux, T. W. Gorczyca, M. S. Pindzola, and N. R. Badnell, Phys. Rev. A **52**, 1319 (1995).
[8] H. L. Zhang and A. K. Pradhan, Phys. Rev. Lett. **78**, 195 (1997).
[9] T. W. Gorczyca and N. R. Badnell, Phys. Rev. Lett. **79**, 2783 (1997).
[10] F. Robicheaux and M. S. Pindzola, Phys. Rev. Lett. **79**, 2237 (1997).
[11] D. C. Griffin, F. Robicheaux, and M. S. Pindzola, Phys. Rev. A **57**, 2708 (1998).
[12] F. Robicheaux, M. S. Pindzola, and D. C. Griffin, Phys. Rev. Lett. **80**, 1402 (1998).
[13] H. Feshbach, Ann. Phys. (N.Y.) **19**, 287 (1962).
[14] Y. Hahn, Adv. At. Mol. Phys. **21**, 123 (1985).
[15] It should be noted here that Eq. (17) for the generalized CA rates in [12] is incorrect and should read $\Gamma^{a,r}_{\rho,\rho'} = \Sigma_{l,m}\Gamma^{a,r}_{nl}U^{*}_{nlm,\rho'}U_{nlm,\rho}$.
[16] D. C. Griffin, M. S. Pindzola, and C. Bottcher, Phys. Rev. A **33**, 3124 (1986).
[17] R. D. Cowan, *The Theory of Atomic Structure and Spectra* (University of California Press, Berkeley, 1981).
[18] T. Bartsch, A. Müller, W. Spies, J. Linkemann, H. Danared, D. R. DeWitt, H. Gao, W. Zong, R. Schuch, A. Wolf, G. H. Dunn, M. S. Pindzola, and D. C. Griffin, Phys. Rev. Lett. **79**, 2233 (1997).